*Inorg. Chem.* **2006**, *45*, 679–687


# $MS_2(Me_2PC_2H_4PMe_2)_2$ (M = Mo, W): Acid–Base Properties, Proton Transfer, and Reversible Protonolysis of Sulfido Ligands

**Steven J. Smith, C. Matthew Whaley, Thomas B. Rauchfuss,* and Scott R. Wilson**

*Department of Chemistry, University of Illinois at Urbana−Champaign, Urbana, Illinois 61801*

Received August 24, 2005

The acid–base reactivity of $MS_2(dmpe)_2$, where M = Mo (**1**) and W (**2**) and dmpe = $Me_2PCH_2CH_2PMe_2$, was examined. Compounds **1** and **2** arise via the one-pot reaction of $(NH_4)_2MS_4$ and dmpe. Protonation of these species gives the stable salts $[MS(SH)(dmpe)_2]X$. The p$K_a$'s of the Mo and W compounds are estimated to be 16.5 and 15.5, respectively. Protonation causes the M═S distances to diverge from 2.24 Å to 2.06 and 2.57 Å, whereas the Mo–P distances do not change appreciably. $^1$H and $^{31}$P NMR studies for [**1**H]$BAr^F_4$ reveal that the proton exchange is competitive with the NMR time scale; at low temperatures, individual signals for both the parent disulfide and its conjugate acid can be observed. Treatment of **1** with excess HOTf liberates $H_2S$ to afford $[MoS(OTf)(dmpe)_2]OTf$, which forms an adduct with $CD_3CN$ and regenerates **1** upon treatment with $SH^-/Et_3N$ solutions. Consistent with its ready protonation, complex **1** is methylated, and the use of excess MeOTf gives $[MoS(OTf)(dmpe)_2]^+$ and $Me_2S$ in a rare example of double alkylation at a sulfido ligand.

## Introduction

In inorganic chemistry, many studies have focused on basicity as it relates to reactions *at* the metal center, e.g., ligand substitution and protonation/alkylation at metals. Fewer studies, however, have systematically examined the basicity and nucleophilicity of coordinated ligands, especially chalcogenide ligands.[1] In this paper, we address this gap through an examination of an important class of metal dichalcogenides.

Starting in 1991, a series of publications have described the 18e, d$^2$ complexes of the type *trans*-$ME_2L_4$, where M = Mo, W and E = S, Se, Te and L = 2e donor ligand (Figure 1). Parkin and co-workers developed $MoS_2(PMe_3)_4$[2] and the corresponding W analogues and Se and Te derivatives thereof.[3] Cotton and co-workers, using $Mo(N_2)_2(diphos)_2$ precursors, prepared the corresponding series $MoE_2(diphos)_2$ for E = O, S, Se, Te (diphos = $Ph_2PCH_2CH_2PPh_2$, *cis*-$Ph_2PCH$═$CHPPh_2$).[4] Yoshida and co-workers described *trans*-$MoS_2(Me_8[16]\text{-aneS}_4)$ via the reaction of *trans*-$Mo(N_2)_2(Me_8[16]\text{-aneS}_4)$ with $S_8$ or *t*-BuSH, where $Me_8[16]\text{-aneS}_4$ is a tetradentate thioether macrocycle.[5] The species "$(C_5H_5)_2MoS$",[6] which is related to the aforementioned series of *trans*-$MoS_2L_4$ complexes in ostensibly being a d$^2$, 18e M═S complex, is unstable and of undefined nuclearity.

These reports comprise the foundation literature for d$^2$ complexes containing "pure" M═E double bonds (E = S, Se, Te). The Mo═S bond lengths are 2.22−2.25 Å vs ∼2.15 Å, typical for the more pervasive bonds between Mo and S that usually have triple-bond character.[7] The bonding in these 18e species has been described using both qualitative and Hartree−Fock molecular orbital theory; the trans geometry is characteristic of the d$^2$ configuration.[4,8] The correlation of bond order and bond lengths is confirmed by Yoshida's characterization of the methylated derivative *trans*-$[MoS(SMe)(Me_8[16]\text{-aneS}_4)]I$, wherein the Mo−S bonds diverge from 2.24 Å to 2.14 and 2.44 Å.[9] Thus, alkylation could be

* To whom correspondence should be addressed. E-mail: rauchfuz@uiuc.edu.

(1) Nugent, W. A.; Mayer, J. M. *Metal−Ligand Multiple Bonds*; John Wiley: New York, 1988.
(2) Murphy, V. J.; Rabinovich, D.; Halkyard, S.; Parkin, G. *J. Chem. Soc., Chem. Commun.* **1995**, 1099−1100.
(3) Rabinovich, D.; Parkin, G. *J. Am. Chem. Soc.* **1991**, *113*, 9421−9422. Rabinovich, D.; Parkin, G. *J. Am. Chem. Soc.* **1991**, *113*, 5904−5905. Rabinovich, D.; Parkin, G. *J. Am. Chem. Soc.* **1993**, *115*, 9822−9823. Rabinovich, D.; Parkin, G. *Inorg. Chem.* **1994**, *33*, 2313−2314. Rabinovich, D.; Parkin, G. *Inorg. Chem.* **1995**, *34*, 6341−6361.
(4) Cotton, F. A.; Schmid, G. *Inorg. Chem.* **1997**, *36*, 2267−2278.
(5) Yoshida, T.; Adachi, T.; Matsumura, K.; Kawazu, K.; Baba, K. *Chem. Lett.* **1991**, 1067−1070.
(6) Pilato, R. S.; Eriksen, K. A.; Stiefel, E. I.; Rheingold, A. L. *Inorg. Chem.* **1993**, *32*, 3799−3800.
(7) Parkin, G. *Prog. Inorg. Chem.* **1998**, *47*, 1−165. Coucouvanis, D. *Adv. Inorg. Chem.* **1998**, *45*, 1−73.
(8) Paradis, J. A.; Wertz, D. W.; Thorp, H. H. *J. Am. Chem. Soc.* **1993**, *115*, 5308−5309.
(9) Yoshida, T.; Adachi, T.; Matsumura, K.; Baba, K. *Chem. Lett.* **1992**, 2447−2450.

10.1021/ic051443c CCC: $33.50 
Published on Web 12/23/2005

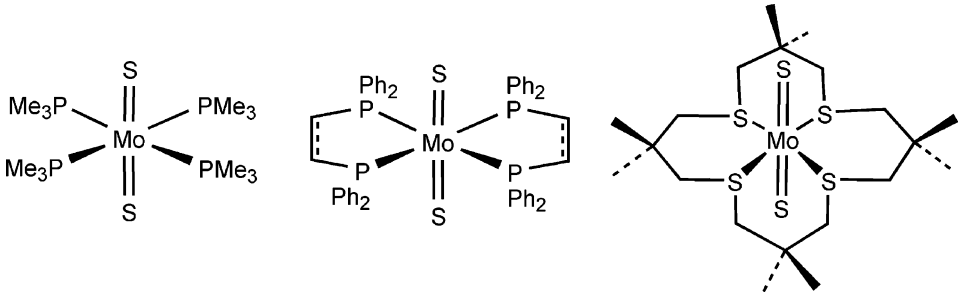

**Figure 1.** Prototypical $d^2$ $MoS_2L_4$ complexes.

described as being "spring-loaded" because of the large structural change that accompanies attachment of the electrophile.

Peripherally related to the focus of this paper, numerous $d^0$ species also feature "pure" M═E double bonds, e.g., $Cp^*_2M(S)(py)$ (M = Ti, Zr, Hf),[10] (triamine)$MoE_3$ (E = O, S),[11] $(C_5Me_5)ReO_3$,[12] $[(C_5Me_5)MoS_3]^-$,[13] and $[Cl_3ReO_3]^{2-}$.[14] These $d^0$ compounds might be expected to display diminished basicity relative to the $d^2$ M═E species. Other interesting 18e M═E species include the cationic $d^4$ oxo-complexes.[15] Compounds with pure M═S/Se/Te bonds may also be viewed as transition-metal representatives of "heavy ketones", defined by Okazaki and Tokitoh to describe M═E-bonded systems where E is S, Se, or Te and M is a main-group atom heavier than the first row.[16] Analogous to the 18e M═E species, the heavy ketones follow the octet rule.

A theme that is relevant to basicity is, of course, the behavior of the conjugate acid. The present cases are, in principle, dibasic because of the presence of two equivalent sites of protonation. Monoprotonation of such dibasic species opens questions of degenerate proton exchange. Little information exists on the proton-exchange dynamics of M−S−H systems, which contrasts with the centrality of Mo−S−H functionalities in catalytic H-atom transfers in both enzymology and industrial hydrotreating catalysis.[17−19] Slow proton transfer has been observed in oxides, such as $Re(O)(OH)(C_2Me_2)_2$,[20] but not in sulfides.

## Results

**Synthesis and Basic Properties of $MoS_2(dmpe)_2$.** Parkin's synthesis of $MoS_2(PMe_3)_4$ involved the intermediacy of $Mo(PMe_3)_6$, prepared via the Na/K reduction of $MoCl_5$/$PMe_3$ mixtures at low temperatures.[21] We recently found that $MoS_2(PMe_3)_4$ forms efficiently upon treatment of MeCN slurries of $(NH_4)_2MoS_4$ with $PMe_3$ at room temperature (eq 1).[22] Reflecting their high basicity (see below), the sulfido ligands in $MoS_2(PMe_3)_4$ resist further desulfurization by $PMe_3$. The coproducts, $H_2S$, $NH_3$, and even $SPMe_3$, are volatile; thus, reaction workup is convenient and efficient. A proton source, in this case $NH_4^+$, is essential to assist in the elimination of $H_2S$.[22] Important to this paper, $MoS_2(dmpe)_2$ (**1**) can be prepared via ligand exchange from $MoS_2(PMe_3)_4$ but also formed via the one-pot reaction of $(NH_4)_2MoS_4$ and 2.5 equiv of dmpe (dmpe = $Me_2PCH_2CH_2PMe_2$, eq 2). We also found that MeCN solutions of either $(NH_4)_2MoS_4$

$$(NH_4)_2MoS_4 + 5PMe_3 \rightarrow MoS_2(PMe_3)_4 + H_2S + 2NH_3 + SPMe_3 \quad (1)$$

$$(NH_4)_2MoS_4 + 2.5dmpe \rightarrow MoS_2(dmpe)_2 + H_2S + 2NH_3 + 0.5dmpeS_2 \quad (2)$$

$MoS_2O_2$ or $(NH_4)_2MoS_3O$, $PMe_3$, and dmpe produce **1** as well. The intensely green species $MoS_2(dmpe)_2$ exhibits good solubility in benzene and THF but is only poorly soluble in MeCN and alkanes. Its solutions can be handled in air, at least briefly, and show no tendency to dissociate ligands in solution.

The analogous violet tungsten complex $WS_2(dmpe)_2$ (**2**) was prepared similarly to the Mo compound. [23] Starting with $(PPh_4)_2MoSe_4$ and using $NH_4PF_6$ as the proton source, we also synthesized the brown-colored $MoSe_2(dmpe)_2$, which was crystallographically characterized.

**Protonation of $MS_2(dmpe)_2$ (M = Mo, W).** Upon the addition of protic acids, green solutions of **1** changed to orange or brown, depending on the strength of the reacting acid. Treating **1** with 1 equiv of methanesulfonic acid


(10) Sweeney, Z. K.; Polse, J. L.; Andersen, R. A.; Bergman, R. G. *Organometallics* **1999**, *18*, 5502−10. Sweeney, Z. K.; Polse, J. L.; Andersen, R. A.; Bergman, R. G. *J. Am. Chem. Soc.* **1998**, *120*, 7825−7834. Howard, W. A.; Parkin, G. *J. Am. Chem. Soc.* **1994**, *116*, 606−615.

(11) Partyka, D. V.; Staples, R. J.; Holm, R. H. *Inorg. Chem.* **2003**, *42*, 7877−7886.

(12) Romao, C. C.; Kuhn, F. E.; Herrmann, W. A. *Chem. Rev.* **1997**, *97*, 3197−3246.

(13) Kawaguchi, H.; Yamada, K.; Lang, J.; Tatsumi, K. *J. Am. Chem. Soc.* **1997**, *119*, 10346−10358. Cao, R.; Tatsumi, K. *Inorg. Chem.* **2002**, *41*, 4102−4104.

(14) Grove, D. E.; Johnson, N. P.; Wilkinson, G. *Inorg. Chem.* **1969**, *8*, 1196.

(15) Meyer, T. J.; Huynh, M. H. V. *Inorg. Chem.* **2003**, *42*, 8140−8160. Bryant, J. R.; Matsuo, T.; Mayer, J. M. *Inorg. Chem.* **2004**, *43*, 1587−1592. Klinker, E. J.; Kaizer, J.; Brennessel, W. W.; Woodrum, N. L.; Cramer, C. J.; Que, L., Jr. *Angew. Chem., Int. Ed.* **2005**, *44*, 3690−3694.

(16) Okazaki, R.; Tokitoh, N. *Acc. Chem. Res.* **2000**, *33*, 625−630.

(17) Stiefel, E. I. *J. Chem. Soc., Dalton Trans.* **1997**, 3915−3923. Stiefel, E. I. *ACS Symp. Ser.* **1996**, *653*, 2−38.

(18) Kuwata, S.; Hidai, M. *Coord. Chem. Rev.* **2001**, *213*, 211−305.

(19) Peruzzini, M.; de los Rios, I.; Romerosa, A. *Prog. Inorg. Chem.* **2001**, *49*, 169−543.

(20) Erikson, T. K. G.; Mayer, J. M. *Angew. Chem., Int Ed. Engl.* **1988**, *100*, 1527−1529. Kramarz, K. W.; Norton, J. R. *Prog. Inorg. Chem.* **1994**, *42*, 1−65.

(21) Murphy, V. J.; Parkin, G. *J. Am. Chem. Soc.* **1995**, *117*, 3522−3528.

(22) Schwarz, D. E.; Rauchfuss, T. B.; Wilson, S. R. *Inorg. Chem.* **2003**, *42*, 2410−2417.

(23) Curtis, C. J.; Miedaner, A.; Ciancanelli, R.; Ellis, W. W.; Noll, B. C.; Rakowski DuBois, M.; DuBois, D. L. *Inorg. Chem.* **2003**, *42*, 216−227.

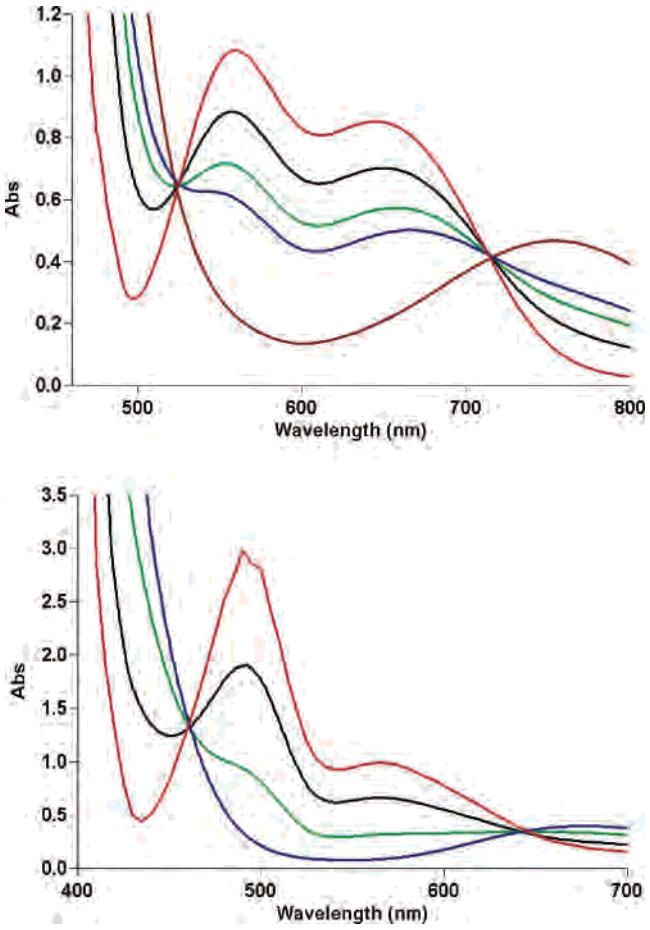


**Figure 2.** Optical spectra for various stages in the protonation of **1** (top) and **2** (bottom) with HOMs in MeCN solution. The aliquot sizes for **1** were 0, 0.25, 0.5, 0.75, and 1.0 mol, and for **2**, the aliquot sizes were 0, 0.3, 0.6, and 1.0 mol.

(HOMs; p$K_a$ = 10.0 in MeCN; all p$K_a$'s are quoted for a MeCN solution unless otherwise noted) gives the bright-orange salt [MoS(SH)(dmpe)$_2$]OMs, [**1**H]OMs. Optical measurements show that this reaction proceeds cleanly with isosbestic points at 530 and 710 nm (Figure 2). The $^1$H NMR spectrum of [**1**H]OMs in a $CD_3CN$ solution consists of a quintet at $\delta$ −4.08 for the $^{31}$P-coupled S*H* group. The methyl groups on the dmpe ligands are inequivalent, whereas the single $^{31}$P NMR signal is consistent with $C_{2v}$ symmetry (Figure 3).

To test the possibility that S protonation would suppress dissociation of phosphine from the otherwise labile $PMe_3$ species, $MoS_2(PMe_3)_4$ was treated with 1 equiv of $H(Et_2O)_2$-$BAr^F_4$ ($Ar^F$ = 3,5-$(CF_3)_2C_6H_3$) in a THF-$d_8$ solution at −70 °C to produce a bright-orange solution. The $^1$H NMR spectrum reveals that protonation occurs analogously to that of **1** with a quintet centered at $\delta$ −2.08 for the $^{31}$P-coupled S*H* and a peak at $\delta$ 1.89 for the four equivalent P*Me*$_3$ groups. Upon warming to room temperature, the S*H* and P*Me*$_3$ signals decreased concomitantly with an increase in the signal for $SPMe_3$. Thus, protonation does not suppress the lability of the $PMe_3$ ligands.

The S*H* NMR signal in [**1**H]OMs disappears upon treatment with $D_2O$. On the basis of its formal 16e configuration, we considered the possibility that [**1**H]$^+$ might undergo exchange with $D_2$, but exposure of either $CD_3CN$ or $CD_3NO_2$ solutions of [**1**H]$BAr^F_4$ to ca. 1 atm of $D_2$ resulted in no change in the $^1$H NMR spectrum after 48 h.

Protonation of **2** with HOMs results in a color change from deep purple to neon green (Figure 2). An equimolar mixture of **1** and [**2**H]OMs in a $CD_3CN$ solution results in a dark-orange solution, the $^{31}$P NMR spectrum of which reveals two broad peaks, one at $\delta$ 29.5 for the average of **1** and [**1**H]OMs and one at $\delta$ 2 for the average of **2** and [**2**H]OMs. Analysis of chemical shifts in this mixture indicates that **1** is more basic than **2**, with a $K_{eq}$ = 10−11 (eq 3).

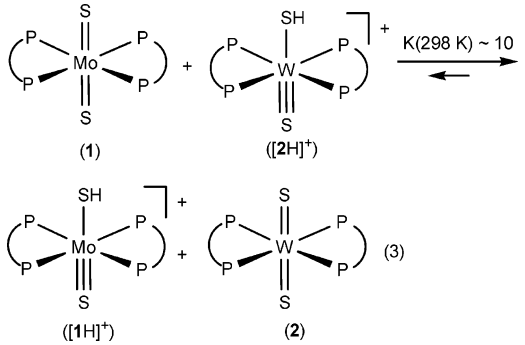


Compound **1** is protonated by $NH_4PF_6$ (p$K_a$ = 16.5) and subsequently deprotonated by $Et_3N$ (p$K_a$ of $Et_3NH^+$ = 18.7),[24] as demonstrated by $^1$H and $^{31}$P NMR spectroscopy. Because **2** is not protonated by $NH_4^+$, i.e., has a p$K_a$ < 16.5, and because it is 10 times more weakly basic than **1**, it follows that the p$K_a$ of **1** is 16.5−17.5.

**Structural Studies on [M(S)(SR)(dmpe)$_2$]$^+$.** Although $MoS_2(Me_8[16]\text{-}aneS_4)$ can be alkylated,[9] its protonation results in immediate elimination of $H_2S$ to give *trans*-$[Mo_2S_3(Me_8[16]\text{-}aneS_4)_2]^{2+}$.[25] Crystallographic characterization of [**1**H]$BAr^F_4$ reveals that protonation most significantly affects the Mo−S bond lengths (Figure 4). In neutral *trans*-$MoS_2(dmpe)_2$, the two Mo═S bonds are 2.250(9) Å in length, whereas in [**1**H]$BAr^F_4$, these distances have diverged to 2.062(7) and 2.573(7) Å. The Mo−P distances do not change appreciably upon protonation; however, the S≡Mo−P bond angles increase from 91.1° to 95.4° as the diphosphine ligands tilt away from the Mo≡S.

Crystallographic results on [**2**H]OMs proved consistent with the results for the Mo derivatives. In neutral $WS_2(PMe_3)_4$, the W═S distance is 2.252 (3) Å, whereas in [**2**H]-OMs, these distances diverge to 2.074(13) and 2.581(13) Å. The S≡W−P bond angles again show that the diphosphine ligands bend away from the more tightly bonded terminal sulfido ligand.

**Proton-Transfer Dynamics.** Preliminary measurements suggested that proton transfer in [**1**H]$^+$ can be sluggish. For example, the $^1$H NMR spectrum of [**1**H]OMs shows two equally intense P*Me* signals, separated by 150 Hz ($\Delta\nu$). On the basis of the relation $\tau = 2^{1/2}\pi(\Delta\nu)$, the rate of site

(24) Izutsu, K. *Acid−Base Dissociation Constants in Dipolar Aprotic Solvents*; Blackwell Scientific Publications: Oxford, U.K., 1990.
(25) Yoshida, T.; Adachi, T.; Matsumura, K.; Baba, K. *Angew. Chem., Int. Ed. Engl.* **1993**, *32*, 1621−1623.

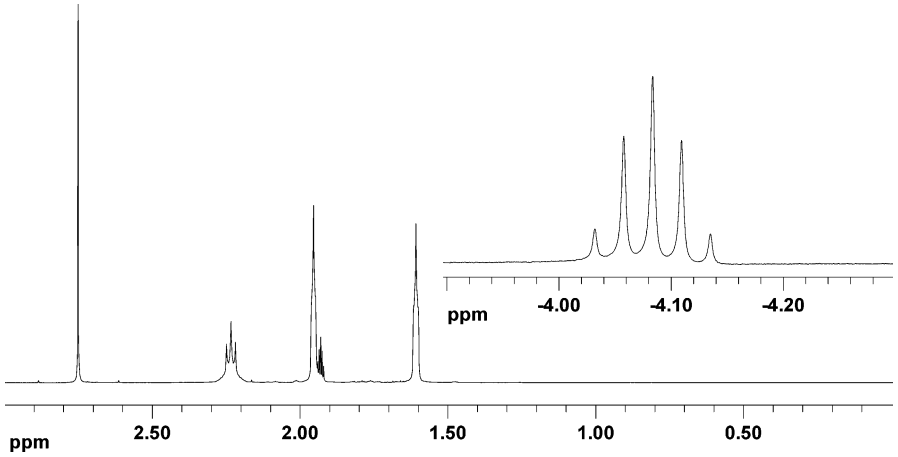


**Figure 3.** 500-MHz $^1$H NMR spectrum of [MoS(SH)(dmpe)$_2$]OMs in a $CD_3CN$ solution. The inset shows the S*H* signal, $J$(P,H) = 13 Hz.

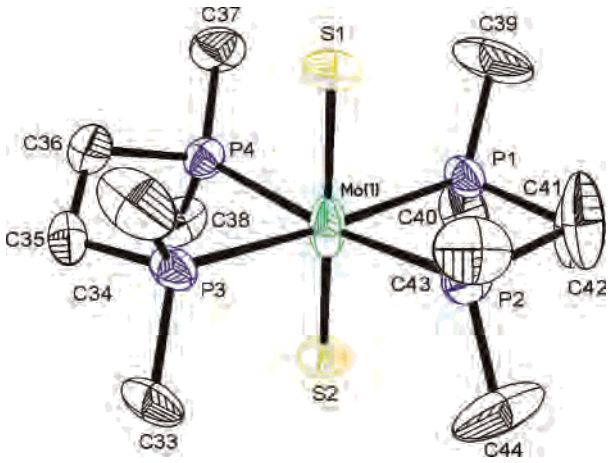


**Figure 4.** Molecular structure of the cation in [MoS(SH)(dmpe)$_2$]BAr$^F_4$ with 50% thermal ellipsoids.

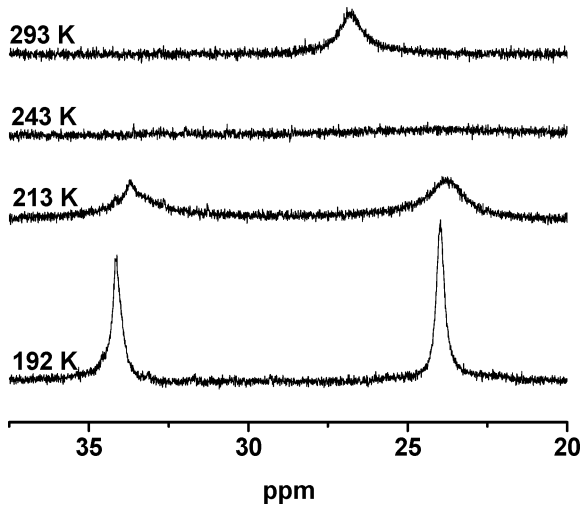


**Figure 5.** 200-MHz $^{31}$P NMR spectra of [MoS(SH)(dmpe)$_2$]BAr$^F_4$ in acetone-$d_6$ at various temperatures.

exchange is $<1000$ s$^{-1}$. Furthermore, the $^{31}$P NMR spectrum of an equimolar solution of [MoS(SH)(dmpe)$_2$]OMs and $MoS_2$(dmpe)$_2$ consists of a broad signal at the average of the singlets for two individual components.

The optical spectrum of the salt with the ostensible formula [**1**H]BAr$^F_4$ indicated the presence of both [**1**H]$^+$ (as for the OMs$^-$ salt) and **1**. The addition of 1 equiv of HOMs converted the brown solution to bright orange, characteristic of pure [**1**H]$^+$. Ambient-temperature $^1$H and $^{31}$P NMR spectra of [**1**H]BAr$^F_4$ in a $CD_3CN$ solution are broadened relative to the corresponding OMs$^-$ salt. Analysis of chemical shifts established that $K_{eq} = 2.3$ at ca. 25 °C. Upon cooling of the sample to −40 °C, the $^{31}$P NMR signal decoalesces to singlets at $\delta$ 22.5 and 32.5, assignable to **1** and [**1**H]$^+$, respectively. Low-temperature (−80 °C) $^{31}$P NMR (Figure 5) analysis indicated that the **1**/[**1**H$^+$] ratio is higher in acetone-$d_6$ vs $CD_3CN$, consistent with the greater basicity[26] of $Me_2CO$.

The $^1$H NMR spectrum of [**2**H]OMs in a $CD_3CN$ solution consists of a broad singlet for the P−methyl groups, suggesting that proton exchange is more rapid for this species vs the Mo analogue (see below). With the less basic solvent $CD_3NO_2$, the $^1$H NMR spectrum of [**2**H]OMs consists of separate peaks for the P−methyl groups, indicating again that the less basic solvent inhibits proton transfer.

**[MoS(OTf)(dmpe)$_2$]$^+$.** Treatment of **1** in a MeCN solution with an excess of HOTf liberated $H_2S$ ($\delta$ 1.05). From the resulting solution, we obtained a high yield of the salt [MoS(OTf)(dmpe)$_2$]OTf ([**3**]OTf) as an analytically pure pale-green solid. The rate of protonolysis of the sulfido ligand is, however, sensitive to the acidity of the acid. The addition of 2 equiv of HOMs (p$K_a = 10.0$)[24] to a $CD_3CN$ solution of **1** liberated $H_2S$ only over the course of several hours.

The $^{19}$F NMR spectrum of [**3**]OTf in a $CD_2Cl_2$ solution showed equally intense signals at $\delta$ −79.7 and −78.0 for free and coordinated OTf$^-$, respectively. In a $CD_3CN$ solution, the $^{19}$F NMR spectrum simplified to a single peak at $\delta$ −79.7, indicating that the MeCN displaced the coordinated triflate. The addition of more than 2 equiv of MeOTf to a MeCN solution of **1** also produced [**3**]OTf, via an unusual example of a double alkylation of a sulfido ligand (see below).

Crystallographic analysis of [**3**]OTf showed that this complex exhibits similarities to [**2**]$^+$ in the Mo≡S bond length and the S−Mo−P bond angles (Tables 1−4). The Mo−O bond length is comparable to those of other Mo(IV) triflate complexes.

(26) Catalán, J.; Diaz, C.; Lopez, V.; Pérez, P.; De Paz, J.-L. G.; Rodriguez, J. G. *Liebigs Ann. Chem.* **1996**, 1785−1794.

**Table 1.** Selected Bond Lengths (Å) and Angles (deg) for **1** and [**1**H]$BAr^F_4$

| | **1** | [**1**H]$BAr^F_4$ |
|---|---|---|
| Mo═S or Mo≡S | 2.2476(9)−2.2497(8) | 2.062(7) |
| Mo−SH | | 2.573(7) |
| Mo−P | 2.476(8)−2.488(8) | 2.491(2) |
| S═Mo−P | 87.64(10)−93.6(4) | 95.38(2) |
| P−Mo−P | 99.45(3) | 98.02(8) |

**Table 2.** Selected Bond Lengths (Å) and Angles (deg) for $WS_2(PMe_3)_4$[3] and [**2**H]OMs

| | $WS_2(PMe_3)_4$ | [**2**H]OMs |
|---|---|---|
| W═S or W≡S | 2.252(3) | 2.074(13) |
| W−SH | | 2.581(13) |
| W−P | 2.50(3) | 2.493(17) |
| S═W−P | 82.8/90.6(1) | 94.34(5) |
| P−W−P | 90.6(1) | 99.0(5) |

**Table 3.** Selected Bond Lengths (Å) and Angles (deg) for [**3**]OTf

| | [MoS(OTf)(dmpe)$_2$]OTf |
|---|---|
| Mo≡S | 2.0867(8) |
| Mo−O | 2.2914(19) |
| Mo−P | 2.5090/2.5318(8) |
| S═Mo−P | 94.85/97.65(3) |
| P−Mo−P | 79.67/100.51(2) |

The protonation of the sulfido ligand in **1** to give [**3**]OTf proved to be fully reversible: the addition of $Et_3N$ to a $CD_3CN$ solution containing $[\mathbf{3}]^+$ and 1 equiv of $H_2S$ gave $[\mathbf{1}H]^+$ over the course of 5 h (eq 4). As discussed above, this $MoSH^+$ species can be further deprotonated with $Et_3N$ to give **1**.

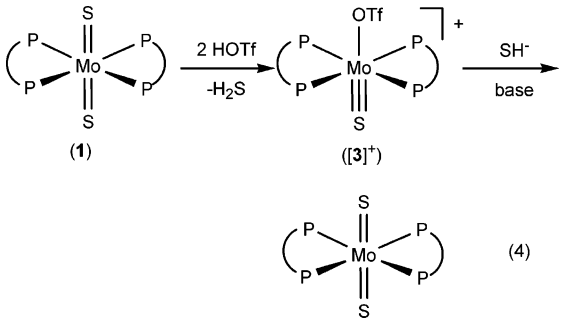


(4)

Further illustrating the displacement of $OTf^-$ by chalcogenides, [**3**]OTf was treated with $PPh_4TeH/Et_3N$ or 2 equiv of $Bu_4NOH$ to give MoS(E)(dmpe)$_2$ (E = O, Te, respectively). Spectroscopic and mass spectrometric data are consistent with the formation of these mixed chalcogenide species.

**Alkylation Studies.** Consistent with its ready protonation, complex **1** is methylated by MeI. Solutions of **1** do not, however, react with PhBr or even $PhCH_2Cl$. Analogous to the protonations, the methylation was signaled by a green-to-orange color change. The $^1$H NMR spectrum of [MoS(SMe)(dmpe)$_2$]I ([**1**Me]I) shows two signals for the PMe groups consistent with the conversion from $D_{2h}$ to idealized $C_{2v}$ symmetry. The SMe group appears as a $^{31}$P-coupled pentet at $\delta$ 1.38. The $^{31}$P NMR spectrum reveals one peak for the four equivalent phosphorus atoms. Yoshida methylated *trans*-$MoS_2(Me_8[16]\text{-aneS}_4)$ with MeI in a similar fashion.[9] Using MeOTf, one can doubly methylate **1** to give high yields of both [**3**]OTf and $Me_2S$ (eq 5).

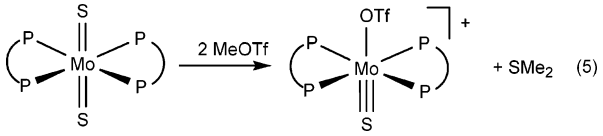


(5)

## Conclusions

Given their distinctive electronic structure and their dramatic structural and electronic responses to S functionalization, the *trans*-$MS_2L_4$ compounds are highly unusual Lewis bases. Their reactivity has received little attention, partially because of synthetic challenges that this and our preceding report[22] resolve. We have shown that a variety of *trans*-$MoE_2(diphos)_2$ species could be prepared with diverse diphosphines and chalcogenides. Because these complexes are relatively kinetically stable, they lend themselves to mechanistic and structural analysis.

**Basicity.** $MoS_2(dmpe)_2$ is a relatively basic metal sulfide. Its basicity exceeds that of the dianion $[MoS_4]^{2-}$, which is not protonated by $NH_4^+$.[22,27] **2** is ca. 10 times *less* basic than $MoS_2(dmpe)_2$. NMR evidence also points to the greater acidity of the WSH versus MoSH complex in terms of more rapid proton exchange and lower field NMR chemical shift for WS*H* vs MoS*H* in [**2**H]OMs and [**1**H]OMs, respectively. In contrast, for protonation *at the metal*, third-row metals are considerably more basic than their lighter congeners; e.g., the p$K_a$ for $HMn(CO)_5$ at 14 is 7 log units lower than that for $HRe(CO)_5$.[28]

The optical properties of metal complexes rarely are as sensitive to protonation as the complexes described in this work. The case of $MoS_2(dmpe)_2$ (and its analogues[29]) is special because the ground electronic state is strongly altered in the conversion from E═$ML_4$═E to [HE−$ML_4$≡E]$^+$. It is also known that the optical properties of these complexes are highly sensitive to the nature of the ligands[8,29] as well as small structural distortions.[30] Optical changes in the attendant protonation are comparable with those associated with methylation at sulfur.

**Slow Proton Transfer in Metal Sulfides.** The proton-transfer reactivity of metal sulfides and sulfhydryl complexes[18,19] is virtually unstudied. It has been reported that a mixture of the d$^2$ dimer $[(C_5R_5)_2Mo_2(S)(SH)(S_2CH_2)]^+$ and its conjugate base undergoes rapid proton exchange on the NMR time scale.[31] The $^{31}$P NMR spectrum of $[Pt_2(PR_3)_4(\mu\text{-}S)(\mu\text{-}SH)]^+$ also indicates fast proton transfer following a slower conversion from $SH_{equatorial}$ to $SH_{axial}$.[32] A potentially interesting case is the d$^0$ sulfide $(C_5Me_4Et)_2Nb(S)(SH)$,[33] although its dynamic properties have not been reported.

(27) Srinivasan, B. R.; Dhuri, S. N.; Näther, C.; Bensch, W. *Inorg. Chim. Acta* **2005**, *358*, 279−287.
(28) Moore, E. J.; Sullivan, J. M.; Norton, J. R. *J. Am. Chem. Soc.* **1986**, *108*, 2257−2263.
(29) Bendix, J.; Bøgevig, A. *Inorg. Chem.* **1998**, *37*, 5992−6001.
(30) Da Re, R. E.; Hopkins, M. D. *Inorg. Chem.* **2002**, *41*, 6973−6985.
(31) Birnbaum, J.; Godziela, G.; Maciejewski, M.; Tonker, T. L.; Haltiwanger, R. C.; Rakowski DuBois, M. *Organometallics* **1990**, *9*, 394−401.
(32) Mas-Ballesté, R.; Aullón, G.; Champkin, P. A.; Clegg, W.; Mégret, C.; Gonzalez-Duarte, P.; Lledós, A. *Chem. Eur. J.* **2003**, *9*, 5023−5035. Aullón, G.; Capdevila, M.; Clegg, W.; González-Duarte, P.; Lledós, A.; Mas-Ballesté, R. *Angew. Chem., Int. Ed.* **2002**, *41*, 2776−2778.

**Table 4.** Details of Data Collection and Structure Refinement for **1**, [**1**H]$BAr^F_4$, [**2**H]OMs, $MoSe_2(dmpe)_2$, $[MoS(OTf)(dmpe)_2]OTf$[a]

| | **1** | [**1**H]$BAr^F_4$ | [**2**H]OMs | $MoSe_2(dmpe)_2$ | $[MoS(OTf)(dmpe)_2]OTf$ |
|---|---|---|---|---|---|
| formula·solvate | $C_{12}H_{32}MoP_4S_2$ | $C_{44}H_{45}BF_{24}MoP_4S_2$ | $C_{15}H_{39}NO_3P_4S_3W$·MeCN | $C_{12}H_{32}MoP_4Se_2$ | $C_{14}H_{32}O_6F_6MoP_4S_3$ |
| cryst size ($mm^3$) | 0.11 × 0.16 × 0.3 | 0.16 × 0.24 × 0.40 | 0.14 × 0.22 × 0.26 | 0.12 × 0.16 × 0.41 | 0.30 × 0.29 × 0.04 |
| space group | $P2_1/c$ | *Pbca* | *Pnma* | $P2_1/n$ | $P2_1/c$ |
| *a* (Å) | 13.214(6) | 19.531(4) | 12.622(4) | 8.801(2) | 19.195(2) |
| *b* (Å) | 12.385(5) | 22.835(4) | 20.482(6) | 12.854(3) | 17.8704(19) |
| *c* (Å) | 13.228(6) | 24.407(5) | 10.506(3) | 9.771(3) | 17.7886(19) |
| α (deg) | 90 | 90 | 90 | 90 | 90 |
| *β* (deg) | 92.733(7) | 90 | 90 | 93.393(5) | 106.791(6) |
| *γ* (deg) | 90 | 90 | 90 | 90 | 90 |
| *V* ($Å^3$) | 2162.6(16) | 10885(4) | 2716.0(14) | 1103.4(5) | 5841.8(11) |
| *Z* | 4 | 8 | 4 | 2 | 8 |
| $D_{calcd}$ (mg $m^{-3}$) | 1.767 | 1.615 | 1.676 | 1.668 | 1.652 |
| $\mu$(Mo Kα) ($mm^{-1}$) | 1.355 | 0.550 | 4.735 | 4.172 | 0.948 |
| reflns measd/indep | 11336/3933 | 83270/10034 | 20377/2568 | 10593/2731 | 139266/14956 |
| restraints/params | 0/295 | 738/841 | 0/142 | 284/258 | 1776/1076 |
| GOF | 1.034 | 1.062 | 1.360 | 1.041 | 1.024 |
| $R_{int}$ | 0.0297 | 0.0989 | 0.0441 | 0.0277 | 0.0422 |
| R1 [$I > 2\sigma(I)$] (all data) | 0.0272 (0.0415) | 0.0557 (0.0986) | 0.0276 (0.0432) | 0.0247 (0.0341) | 0.0368 (0.0504) |
| wR2 [$I > 2\sigma(I)$] (all data) | 0.0645 (0.0699) | 0.1440 (0.1602) | 0.0683 (0.1001) | 0.0610 (0.0640) | 0.0917 (0.1007) |
| max peak/hole ($e^-/Å^3$) | 0.618/−0.434 | 0.909/−0.559 | 0.678/−1.227 | 0.328/−0.446 | 1.328/−1.375 |

[a] $R1 = \Sigma||F_o| - |F_c||/\Sigma|F_o|$; $wR2 = \{\Sigma[w(F_o^2 - F_c^2)^2]/\Sigma[w(F_o^2)^2]\}^{1/2}$.

The slow proton transfer in $[MoS(SH)(dmpe)_2]^+$ is consistent with a substantial energetic barrier associated with rehybridization of $L_4Mo(=S)_2$ into $[L_4Mo(\equiv S)(-SH)]^+$. Structural studies bear this out; protonation causes the two Mo=S bond lengths of 2.24 Å to diverge to 2.06 and 2.57 Å, characteristic of triple and single bonds, respectively (eq 6).

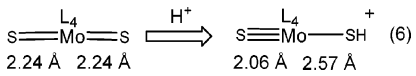

(6)

In $[MoS(SMe)(Me_8[16]\text{-}aneS_4)]^+$, the Mo−S distances are also divergent at 2.14 and 2.44 Å vs ∼2.24 Å in the parent *trans*-$MoS_2(Me_8[16]\text{-}aneS_4)$.[9] Kubas has reported an Mo−SH distance of 2.596(3) Å in the alkylidyne complex *trans*-$Mo(SH)(\equiv CNMe_2)(dppe)_2$.[34] In $[Mo(SH)O(Me_8[16]\text{-}aneS_4)]^+$, the Mo−SH distance is 2.49 Å.[35]

**Protonolysis and Methylation Reactions.** *trans*-$MoS_2(dmpe)_2$ undergoes sequential double protonation or double methylation at the same S atom. In a related finding, Bendix and Bøgevig reported that $MO_2(dppe)_2$ (M = Mo, W) reacts with excess acid to give $[MO(X)(dppe)_2]^+$ (X = Cl, Br, I, OMe).[29] The second protonation of $[MoS(SH)(dmpe)_2]^+$ occurs at *S*H. The sequential alkylation and protonation at a sulfido ligand is a potentially useful method for the synthesis of thiols. The advantages to the use of $MoS_2L_4$ complexes for this transformation are that thioether formation is noncompetitive and the spent molybdenum reagent can be recycled. The reactivity of $MoS_2(dmpe)_2$ toward common alkylating agents is, however, too low for practical use. Presently, however, $MoS_2(dmpe)_2$ is insufficiently reactive toward common alkylating agents.

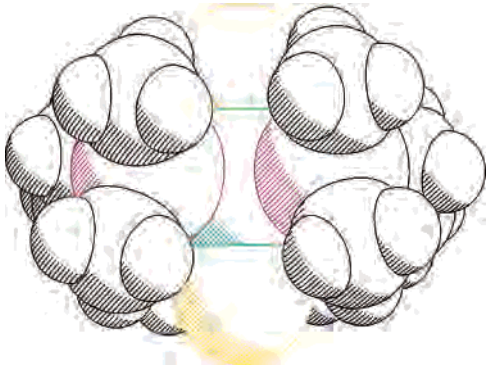

**Figure 6.** Space-filling model of $MoS_2(dmpe)_2$.

In contrast to the apparent instability of $[MoS(SH)(Me_8\text{-}[16]\text{-}aneS_4)]^+$,[25] $[MoS(SH)(dmpe)_2]^+$ is stable with respect to loss of $H_2S$. This enhanced stability may reflect the steric protection afforded by the four P−Me groups that project above and below the $MoP_4$ plane (Figure 6).

**$[MoS(dmpe)_2]^{2+}$, an Unusual 16e, $\pi$ Acid.** 16e fragments have played useful roles in coordination chemistry, e.g., $[Ru(NH_3)_5]^{2+}$, $[CpFe(CO)_2]^+$, $Mo(CO)_5$, etc. These metal electrophiles are, however, all $\pi$ bases reflecting their $d^6$ configuration. In contrast, $[MS(dmpe)_2]^{2+}$ (M = Mo, W) is a $\pi$ acid, which suggests that it will be a novel platform for examining $\pi$-basic ligands. The unusual character of $[MS(dmpe)_2]^{2+}$ is illustrated by its ability to accept $S^{2-}$ to reform M=E bonds, i.e., $M-OTf^+ \rightarrow M{=}S$. Halide complexes can often be converted to the corresponding SH derivatives,[19] i.e., step i in eq 7, but their further conversion into terminal sulfido ligands remains otherwise unprecedented.

$$[L_nM-X]^+ \xrightarrow[i]{SH^-} [L_nM-SH]^+ \xrightarrow[ii]{-H^+} L_nM{=}S \qquad (7)$$

## Experimental Section

**General Procedures.** As previously described,[22] synthetic reactions were conducted under a flowing $N_2$ atmosphere. The following reagents were synthesized by published procedures: $(NH_4)_2MoS_4$

(33) Brunner, H.; Gehart, G.; Meier, W.; Wachter, J.; Nuber, B. *J. Organomet. Chem.* **1993**, *454*, 117−122.
(34) Luo, X. L.; Kubas, G. J.; Burns, C. J.; Butcher, R. J. *Organometallics* **1995**, *14*, 3370−3376.
(35) DeSimone, R. E.; Glick, M. D. *Inorg. Chem.* **1978**, *17*, 3574−3577.

and $(NH_4)_2WS_4$,[36] $NaBAr^F_4$ and $H(Et_2O)_2BAr^F_4$,[37] $(PPh_4)_2MoSe_4$,[38] and $MoS_2(PMe_3)_4$.[22] Electronic and IR spectra were recorded on Varian Cary 50Bio and Mattson Infinity Gold FTIR spectrophotometers, respectively.

***trans*-$MoS_2(dmpe)_2$ (1).** A slurry of 0.500 g (1.92 mmol) of $(NH_4)_2MoS_4$ in 10 mL of MeCN was treated with 0.642 mL (3.85 mmol) of dmpe. The solution was frozen, evacuated, and then treated with 0.7 mL (6.77 mmol) of $PMe_3$, which was condensed onto the frozen slurry. *Note:* the low solubility of $(NH_4)_2MoS_4$ in MeCN, along with the prompt freezing of the solution with dmpe limits desulfurization by the chelating phosphine. The mixture was allowed to warm to room temperature and stirred for 4 h. After the resulting green slurry was purged for 1 h, solvent was removed via a cannula and the microcrystals were washed with ca. 10 mL of MeCN. X-ray-quality crystals were grown by cooling the mother liquor at −20 °C. Yield: 300 mg (34%). An additional 130 mg of product can be obtained by cooling the washings to −20 °C for a combined yield of 430 mg (50%). $^1$H NMR ($C_6D_6$): $\delta$ 1.56 (t, 8H, $CH_2$, $J_{PH}$ = 7 Hz), 1.53 (s, 24H, $CH_3$). $^{31}P\{^1H\}$ ($C_6D_6$): $\delta$ 22. IR (KBr, cm$^{-1}$): $\nu_{MoS}$ = 414 (s). ESI(+) MS (MeCN): $m/z$ = 462.9 [$MoS_2(dmpe)_2^+$]. UV−vis (MeCN): $\lambda_{max}$ ($\epsilon$) = 756 (47), 646 (85), 559 (108), 376 (26 800), 254 (12 160), 228 nm (17 820 L mol$^{-1}$ cm$^{-1}$). Anal. Calcd for $C_{12}H_{32}MoP_4S_2$ (found): C, 31.31 (31.29, 31.31); H, 7.01 (7.12, 7.01); Mo, 20.84 (20.90); P, 26.91 (25.34); S, 13.93 (14.21). The basicity of **1** was approximated by the following NMR experiment: ∼20 mg of **1** was treated with a solution of ∼7 mg of $NH_4PF_6$ in 1 mL of $CD_3CN$ to give an orange solution, showing signals assigned (see below) to [**1**H]$^+$. The addition of ∼6 $\mu$L of $Et_3N$ to this solution restored the green color and $^1$H NMR signals characteristic of **1**.

***trans*-$WS_2(dmpe)_2$ (2).** A slurry of 0.300 g (0.862 mmol) of $(NH_4)_2WS_4$ in 10 mL of MeCN was treated with 0.432 mL (2.59 mmol) of dmpe. After stirring for 1 h, the resulting purple solution was filtered, and the solvent was removed in vacuo. The solid was extracted with 10 mL of benzene; this extract was filtered, and the solvent was removed in vacuo. The solid was recrystallized by dissolution in a minimum amount of MeCN at room temperature followed by cooling to −20 °C for 18 h to afford purple microcrystals. Yield: 0.042 g (0.175; 9%). $^1$H NMR ($C_6D_6$): $\delta$ 1.65 (s, 24H, $CH_3$), 1.50 (t, 8H, $CH_2$, $J_{PH}$ = 6.5 Hz). $^{31}P\{^1H\}$ NMR ($C_6D_6$): $\delta$ −0.5 [s and d, $J(^{31}P,^{183}W)$ = 264.2 Hz]. Anal. Calcd for $C_{12}H_{32}P_4S_2W$ (found): C, 26.29 (26.52); H, 5.88 (5.77).

***trans*-$MoSe_2(dmpe)_2$.** To a suspension of 0.300 g (0.275 mmol) of $(PPh_4)_2MoSe_4$ in 7 mL of MeCN was added 0.058 g (0.551 mmol) of $NH_4BF_4$. The solution was frozen, evacuated, and then treated with 0.2 mL (1.93 mmol) of $PMe_3$, which was condensed onto the frozen slurry. The mixture was allowed to warm to room temperature and stirred for 10 min, at which point a brown solution forms and 92 $\mu$L (0.551 mmol) of dmpe was added. The solution was stirred under an $N_2$ purge for 20 min. The solvent was removed in vacuo, and the solid was extracted with 20 mL of $Et_2O$ and filtered. The solvent was removed in vacuo, and the solid was recrystallized from a saturated MeCN solution at −20 °C. X-ray-quality crystals were grown by cooling a saturated MeCN solution to −20 °C. Yield: 0.038 g (25%). $^1$H NMR ($C_6D_6$): $\delta$ 1.61 (s, 24H, $CH_3$), 1.58 (t, 8H, $CH_2$). $^{31}P\{^1H\}$ NMR ($C_6D_6$): $\delta$ 19.0 (s). ESI(+) MS (MeCN): $m/z$ = 555.1 [$MoSe_2(dmpe)_2^+$]. Anal. Calcd for $C_{12}H_{32}MoP_4Se_2$ (found): C, 26.01 (25.79); H, 5.82 (5.44).

(36) McDonald, J. W.; Friesen, G. D.; Rosenhein, L. D.; Newton, W. E. *Inorg. Chim. Acta* **1983**, *72*, 205−210.
(37) Reger, D. L.; Little, C. A.; Lamba, J. J. S.; Brown, K. J. *Inorg. Synth.* **2004**, *34*, 5−8.
(38) Howard, K. E.; Rauchfuss, T. B.; Wilson, S. R. *Inorg. Chem.* **1988**, *27*, 1710−1716.

***trans*-[MoS(SH)(dmpe)$_2$]OMs ([1H]OMs).** A solution of 0.158 g (0.343 mmol) of **1** in 13 mL of MeCN was treated with 23 $\mu$L (0.343 mmol) of HOMs. The resulting bright orange solution was concentrated to ca. 5 mL, and 15 mL of $Et_2O$ was added to precipitate an orange solid, which was washed with 20 mL of $Et_2O$. Yield: 0.178 g (93%). $^1$H NMR ($CD_3CN$): $\delta$ 2.75 (s, 3H, $MeSO_3$), 2.23 (t, 8H, $CH_2$, $J_{PH}$ = 7.5 Hz), 1.95 (s, 12H, $CH_3$), 1.61 (s, 12H, $CH_3$), −4.08 (p, 1H, SH, $J_{PH}$ = 13 Hz). $^{31}P\{^1H\}$ NMR (MeCN-$d_3$): $\delta$ 31.9. IR (KBr, cm$^{-1}$): $\nu_{SH}$ = 2562 (w). UV−vis (MeCN): $\lambda_{max}$ ($\epsilon$) = 756 (47), 430 (2590), 383 nm (2050 L mol$^{-1}$ cm$^{-1}$). Anal. Calcd for $C_{13}H_{36}MoO_3P_4S_3$ (found): C, 28.06 (27.94); H, 6.52 (6.46).

***trans*-[MoS(SH)(dmpe)$_2$]OTf ([1H]OTf).** To a solution of 0.353 g (0.767 mmol) of **1** in 30 mL of $Et_2O$ was added a solution of 68 $\mu$L (0.767 mmol) of HOTf in 10 mL of $Et_2O$. The resulting bright yellow solid was collected and washed with 10 mL of $Et_2O$. Yield: 0.416 g (89%). $^1$H NMR ($CD_3CN$): $\delta$ 2.23 (t, 8H, $CH_2$, $J_{PH}$ = 7.5 Hz), 1.95 (s, 12H, $CH_3$), 1.61 (s, 12H, $CH_3$), −4.08 (p, 1H, SH, $J_{PH}$ = 13 Hz). $^{31}P\{^1H\}$ NMR (MeCN-$d_3$): $\delta$ 31.9. Anal. Calcd for $C_{13}H_{33}F_3MoO_3P_4S_3$ (found): C, 25.58 (25.72); H, 5.45 (5.48).

***trans*-[MoS(SH)(dmpe)$_2$]$BAr^F_4$ ([1H]$BAr^F_4$).** To a solution of 0.175 g (0.38 mmol) of **1** in 20 mL of $Et_2O$ was added a solution of 0.382 g (0.38 mmol) of $H(Et_2O)_2BAr^F_4$ in 8 mL of $Et_2O$. The volume of the resulting rust-colored solution was concentrated to ca. 10 mL under vacuum. Using a cannula, solvent was removed from the rust-colored solid. X-ray-quality crystals were grown from a saturated $Et_2O$ solution at −20 °C. Yield: 0.300 g (60%). $^1$H NMR ($CD_3CN$): $\delta$ 7.68 (s, 12H, Ph), 7.66 (s, 4H, Ph), 2.09 (s, 8H, $CH_2$), 1.70 (s, 24H, $CH_3$), −4.08 (s, 1H, SH). $^{31}P\{^1H\}$ NMR ($CD_3CN$): $\delta$ 30. UV−vis (MeCN): $\lambda_{max}$ ($\epsilon$) = 704 (77), 376 nm (2670 L mol$^{-1}$ cm$^{-1}$). Analysis of chemical shifts established $K_{eq}$ = 2.3 at ca. 25 °C in a $CD_3CN$ solution. The equilibrium constant was determined by the percent shift of the $^{31}$P NMR signal versus that for **1** and [**1**H]$^+$.

***trans*-[WS(SH)(dmpe)$_2$]OMs ([2H]OMs).** To a deep purple solution of 0.078 g (0.142 mmol) of **2** in 5 mL of MeCN was added 9.2 $\mu$L (0.142 mmol) of HOMs. The addition of 15 mL of $Et_2O$ to the resulting neon-green solution gave a bright-green precipitate. After removal of the solvent using a cannula, the solid was washed with 20 mL of $Et_2O$. X-ray-quality crystals were grown by dissolving 0.070 g of the solid in 3 mL of MeCN and then adding 6 mL of $Et_2O$, filtering, and storing the mixture at −20 °C overnight. Yield: 0.082 g (90%). $^1$H NMR ($CD_3CN$): $\delta$ 2.40 (s, 3H, $MeSO_3$), 2.12 (t, 8H, $CH_2$, $J_{PH}$ = 7 Hz), 1.88 (s, 24H, $CH_3$), −3.7 (1H, quintet). $^{31}P\{^1H\}$ NMR (MeCN-$d_3$): $\delta$ 8.4 [s and d, $J(^{31}P,^{183}W)$ = 251 Hz]. The relative p$K_a$ of **1** vs [**2**H]OMs was determined in a competition experiment in a sealable NMR tube fitted with a Teflon screwcap. In a typical experiment, an equimolar mixture of 0.005 g (0.0109 mmol) of **1** and 0.007 g (0.0109 mmol) of the competing acid was dissolved in ∼0.8 mL of $CD_3CN$. The equilibrium constant was obtained by the percent shift of $^{31}$P NMR peaks from **1** toward [**1**H]$^+$. The analogous *trans*-[WS(SH)(dmpe)$_2$]$BAr^F_4$ ([**2**H]$BAr^F_4$) was prepared similarly by treatment of a suspension of 0.070 g (0.128 mmol) of **2** in 10 mL of $Et_2O$ with a solution of 0.110 g (0.128 mmol) of $H(Et_2O)_2BAr^F_4$ in 10 mL of $Et_2O$. Concentration of the resulting homogeneous brown-green solution to ca. 10 mL (0.035 g) precipitated a light-green solid, which was washed with hexane. An additional 0.030 g was isolated upon cooling of the filtrate to −20 °C for a total yield of 0.065 g (36%). Anal. Calcd for $C_{44}H_{45}BF_{24}P_4S_2W$ (found): C, 37.42 (37.57); H, 3.21 (3.12).

***trans*-[MoS(OTf)(dmpe)$_2$]OTf ([3]OTf).** To a deep-green solution of 0.091 g (0.198 mmol) of **1** in 14 mL of MeCN was added

40 μL (0.415 mmol) of HOTf in 10 mL of MeCN over the course of 1 min. During the addition, the solution quickly became orange followed by pale green. The solution was stirred under a slow $N_2$ purge for 30 min and then concentrated to ca. 2 mL. The addition of 8 mL of $Et_2O$ precipitated a green oil. The solvent was decanted via a cannula, and the oil was washed with 20 mL of $Et_2O$. Drying under vacuum yielded a light-green solid. X-ray-quality crystals were grown by vapor diffusion of hexane into a dichloromethane solution. Yield: 0.130 g (90%). $^1$H NMR ($CD_3CN$): $\delta$ 2.42 (s, 8H, $CH_2$), 2.16 (s, 12H, $CH_3$), 1.63 (s, 12H, $CH_3$). $^{31}$P{$^1$H} NMR ($CD_3CN$): $\delta$ 37.5. $^{19}$F NMR ($CD_3CN$): $\delta$ −79.7. $^{19}$F NMR ($CD_2Cl_2$): $\delta$ −78.0, −79.7. $^1$H NMR ($CD_2Cl_2$): $\delta$ 2.43 (br m, 8H, $CH_2$), 2.13 (s, 12H, $CH_3$), 1.82 (s, 12H, $CH_3$). $^{31}$P{$^1$H} NMR ($CD_2Cl_2$): $\delta$ 37.0. $^{19}$F NMR ($CD_2Cl_2$): $\delta$ −78.0, −79.7. ESI(+) MS (MeCN): $m/z$ = 579 [MoS(OTf)(dmpe)$_2^+$], 235.5 [MoS(MeCN)(dmpe)$_2^+$], 215.0 [MoS(dmpe)$_2^{2+}$]. Anal. Calcd for $C_{14}H_{32}F_6MoO_6P_4S_3$ (found): C, 23.15 (23.43); H, 4.44 (4.32).

**(i) Conversion of [3]OTf into 1.** in an NMR tube with a Teflon screwcap, a frozen slurry of 19 mg (0.041 mmol) of **1** and 1 mL of $CD_3CN$ was treated with 13 μL (0.151 mmol) of HOTf. The frozen mixture was evacuated, sealed, and examined by NMR spectroscopy. The reaction was complete upon warming to room temperature as shown by $^1$H and $^{31}$P NMR spectroscopies, which showed the presence of $H_2S$ and [MoS($CD_3CN$)(dmpe)$_2$]$^+$. The solution was then refrozen and treated with 30 μL of $Et_3N$. The frozen mixture was evacuated and allowed to warm to ambient temperatures. $^1$H and $^{31}$P NMR measures showed that the signals for [**1**H]$^+$ formed over the course of 5 h.

**(ii) Reaction of 1 with 2 equiv of MeOTf.** The addition of 0.98 mL of a 0.0884 M solution of MeOTf in $CD_3CN$ was added to 0.020 g (0.043 mmol) of **1**. The $^1$H and $^{31}$P NMR spectra indicated clean conversion to [**3**]OTf. The volatile components were vacuum transferred from the light-green solution into a sealable NMR tube. $^1$H NMR analysis showed the formation of $Me_2S$.

**Generation of MeSPr from 1.** To a solution of 0.150 g (0.326 mmol) of **1** in 15 mL of THF was added 0.318 mL (0.326 mmol) of PrI. The solution darkened to an orange-brown color and was allowed to stir for 16 h while protected from light. The resulting dark-orange suspension was concentrated to ca. 5 mL, and the solid was filtered off and washed with 40 mL of $Et_2O$. Yield: 0.184 g (0.293 mmol, 90%). $^1$H NMR ($CD_3CN$): $\delta$ 2.26 (t, 8H), 1.88 (s, 12H), 1.79 (t, 2H), 1.68 (s, 12H), 1.07 (m, 2H), 0.65 (t, 3H). $^{31}$P NMR ($CD_3CN$): $\delta$ 28.7. The iodide was converted to the $BAr^F{}_4^-$ salt by the addition of 0.260 g (0.293 mmol) of $NaBAr^F{}_4$ to a solution of the iodide salt in 10 mL of MeCN. The mixture was stirred for 10 min before being evaporated. The solid was extracted into 30 mL of $Et_2O$ and filtered. Evaporation of the extract produced an orange powder. Yield: 0.360 g (0.264 mmol, 90%). $^1$H NMR ($CD_3CN$): $\delta$ 7.7 (m, 12H, $BAr^F{}_4$), 2.29 (s, 8H), 1.91 (s, 12H), 1.83 (t, 2H), 1.71 (s, 12H), 1.11 (m, 2H), 0.69 (t, 3H). $^{31}$P NMR ($CD_3CN$): $\delta$ 27.7. An NMR tube was charged with 0.020 g of [MoS(SPr)(dmpe)$_2$]$BAr^F{}_4$ and 0.5 mL of $CD_3CN$ followed by 0.165 mL of 0.0884 M MeOTf in $CD_3CN$. $^1$H NMR ($CD_3CN$): $\delta$ 7.7 (m, 12H, $BAr^F{}_4$), 2.80 (s, 3H), 2.47 (s, 8H), 2.19 (s, 12H), 1.79 (m, 2H), 1.67 (s, 12H), 1.05 (m, 5H). $^{31}$P NMR ($CD_3CN$): $\delta$ 37.5.

**Generation of *trans*-MoS(E)(dmpe)$_2$ (E = O, Te).** To a light-green solution of 0.070 g (0.096 mmol) of [**3**]OTf in 5 mL of MeCN was added 0.193 mL of a 1.0 M solution of $Bu_4NOH$ in MeOH. The solution quickly turned deep purple and then purple/orange. The solvent was removed under reduced pressure to dryness. The addition of 20 mL of $Et_2O$ followed by filtration resulted in a deep-orange solution. Removal of the solvent to dryness produced an orange oil contaminated by $Bu_4N^+$ salts. $^1$H NMR ($C_6D_6$): $\delta$ 1.8−1.6 (m, 8H, $CH_2$), 1.44 (s, 12H, $CH_3$), 1.23 (s, 12H, $CH_3$). $^{31}$P{$^1$H} NMR ($C_6D_6$): $\delta$ 24.8. ESI(+) MS (MeCN): $m/z$ = 447.3 [MoSO(dmpe)$_2^+$]. An analogous experiment using 50 μL of $Et_3N$ and $PPh_4TeH$[39] afforded a dark-red solid. $^1$H NMR ($C_6D_6$): $\delta$ 1.8 (s, 12H, $CH_3$), 1.73 (m, 8H, $CH_2$), 1.5 (s, 12H, $CH_3$). $^{31}$P{$^1$H} NMR ($C_6D_6$): $\delta$ 16. ESI(+) MS (MeCN): $m/z$ = 558.1 [MoSTe(dmpe)$_2^+$].

***trans*-[MoS(SMe)(dmpe)$_2$]I ([1Me]I).** To a solution of 0.250 g (0.543 mmol) of **1** in 10 mL of THF was added 37.3 μL (0.598 mmol) of MeI. The solution immediately assumed a dark-orange color, and orange microcrystals precipitated. After removal of the solvent via a cannula, the solid was washed with 20 mL of $Et_2O$. Yield: 0.304 g (93%). $^1$H NMR ($CD_3CN$): $\delta$ 2.27 (t, 8H, $CH_2$, $J_{PH}$ = 7 Hz), 1.89 (s, 12H, $CH_3$), 1.68 (s, 12H, $CH_3$), 1.39 (quintet, 3H, SMe, $J_{PH} \sim$ 1 Hz). $^{31}$P{$^1$H} NMR ($CD_3CN$): $\delta$ 29.3. UV−vis (MeCN): $\lambda_{max}$ ($\epsilon$) = 438 (3280), 376 (3410), 244 nm (19 900 L mol$^{-1}$ cm$^{-1}$). Anal. Calcd for $C_{13}H_{35}IMoP_4S_2$ (found): C, 25.92 (26.19); H, 5.86 (5.47).

**Crystallography.** Crystals of **1**, $MoSe_2(dmpe)_2$, [**1**H]$BAr^F{}_4$, [**2**H]OMs, and [MoS(OTf)(dmpe)$_2$]OTf were mounted on thin glass fibers by using oil (Paratone-N, Exxon) before being transferred to the diffractometer. Data were collected on a Siemens CCD automated diffractometer at 193 K. Data processing was performed with the integrated program package SHELXTL.[40] Selected aspects of the refinement are discussed below.

**(i) $MoS_2(dmpe)_2$ (1).** Systematic conditions suggested the unambiguous space group, and the structure was phased by direct methods. The proposed model imposed inversion symmetry on the two independent Mo sites and includes one chelate ligand disordered over two sites for Mo1. Chemically similar bond lengths and bond angles for disordered sites were restrained equivalent values with effective standard deviations (esd's) of 0.01 and 0.02 Å, respectively. Displacement parameters for overlapping disordered sites were restrained to be similar (esd 0.01). Methyl H-atom positions were optimized by rotation about P−C bonds with idealized C−H, C···H, and H···H distances. The remaining H atoms were included as riding idealized contributors. Methyl H-atom *U*'s were assigned as 1.5 times $U_{eq}$ of the adjacent atom; the remaining H-atom *U*'s were assigned as 1.2 times the adjacent $U_{eq}$. The space group choice was confirmed by successful convergence of the full-matrix least-squares refinement on $F^2$. The highest peaks in the final difference Fourier map were near S1 and S2; the final map had no other significant features. A final analysis of the variance between observed and calculated structure factors showed little dependence on amplitude or resolution.

**(ii) $MoSe_2(dmpe)_2$.** Systematic conditions suggested the unambiguous space group, and the structure was phased by direct methods. The proposed model imposed inversion symmetry on coordinated Se and dmpe ligands disordered over three sites. Owing to high correlation coefficients, the C1−C2 bond length was idealized using an esd of 0.01 Å, and the chemically similar disordered ligands were restrained to similar geometry (esd 0.01). Anisotropic displacement parameters for superimposed sites were restrained to have similar rigid-bond values. Methyl H-atom positions were optimized by rotation about R−C bonds with idealized C−H, R···H, and H···H distances. The remaining H atoms were included as riding idealized contributors. Methyl H-atom *U*'s were assigned as 1.5 times $U_{eq}$ of the adjacent atom; the remaining H-atom *U*'s were assigned as 1.2 times the adjacent $U_{eq}$. The space

(39) Houser, E. J.; Rauchfuss, T. B.; Wilson, S. R. *Inorg. Chem.* **1993**, *32*, 4069−4076.
(40) Sheldrick, G. M. *SHELXTL*; Bruker AXS: Madison, WI, 1998.

group choice was confirmed by successful convergence of the full-matrix least-squares refinement on $F^2$. The highest peaks in the final difference Fourier map were near C16, Se1, and Se2; the final map had no other significant features. A final analysis of the variance between observed and calculated structure factors showed no dependence on the amplitude or resolution.

**(iii) [MoS(SH)(dmpe)$_2$]BAr$^F_4$ ([1H]BAr$^F_4$).** Systematic conditions suggested the unambiguous space group, and the structure was solved by direct methods. Inversion symmetry was imposed on the proposed model, and the Mo atom was disordered above and below the base plane of the complex. Six $CF_3$ groups for the anion were disordered about the mirror plane. Methyl H-atom *U*'s were assigned as 1.5 times $U_{eq}$ of the corresponding methyl C atom. The remaining H atoms were included as riding idealized contributors with *U*'s assigned as 1.2 times $U_{eq}$ of the adjacent non-H atoms. The space group choice was confirmed by successful convergence of the full-matrix least-squares refinement on $F^2$. The highest peaks in the final difference Fourier map were near S1 and S2; the final map had no other significant features. A final analysis of the variance between observed and calculated structure factors showed no dependence on the amplitude or resolution.

**(iv) [WS(SH)(dmpe)$_2$]OMs ([2H]OMs).** Systematic conditions suggested the ambiguous space group, and the structure was solved by direct methods. Inversion symmetry was imposed on the proposed model, and the W atom was disordered above and below the base plane of the complex. H atoms for the MeCN solvate were disordered about the mirror plane. MeCN and other Me−P H-atom positions of the mirror were optimized by rotation about R−C bonds with idealized C−H, R···H, and H···H distances. Methyl H-atom *U*'s were assigned as 1.5 times $U_{eq}$ of the corresponding methyl C atom. The remaining H atoms were included as riding idealized contributors with *U*'s assigned as 1.2 times $U_{eq}$ of the adjacent non-H atoms. The space group choice was confirmed by successful convergence of the full-matrix least-squares refinement on $F^2$. The highest peak in the final difference Fourier map was near S2; the final map had no other significant features. A final analysis of the variance between observed and calculated structure factors showed no dependence on the amplitude or resolution.

**(v) [MoS(OTf)(dmpe)$_2$]OTf.** Systematic conditions suggested the unambiguous space group, and the structure was phased by direct methods. The proposed model included disordered sites for one of two cations and both anions. The model for the disordered cation included two sites for each chelate ligand and three sites for the axial triflate ligand. Each disordered anion was refined over two sites. Chemically equivalent 1,2 and 1,3 distances for disordered sites were restrained to equal values using esd's of 0.02 and 0.03 Å, respectively. The triflate anions were idealized (esd 0.02 Å). Rigid-bond restraints (esd 0.01) were imposed on displacement parameters for disordered sites. Disordered sites separated by less than 1.7 Å were further restrained to have similar values. Methyl H-atom positions, R−$CH_3$, were optimized by rotation about R−C bonds with idealized C−H, R−H, and H−H distances. The remaining H atoms were included as riding idealized contributors. Methyl H-atom *U*'s were assigned as 1.5 times $U_{eq}$ of the adjacent atom; the remaining H-atom *U*'s were assigned as 1.2 times the adjacent $U_{eq}$. The space group choice was confirmed by successful convergence of the full-matrix least-squares refinement on $F^2$. The highest peaks in the final difference Fourier map were in the vicinity of Mo atoms and the disordered anions; the final map had no other significant features. A final analysis of the variance between observed and calculated structure factors showed little dependence on the amplitude or resolution.

**Acknowledgment.** This research was supported by the National Science Foundation and the Department of Energy. We thank Cameron Spahn for his help with refinements of the crystallographic data.

**Supporting Information Available:** X-ray crystallographic data for of **1**, $MoSe_2(dmpe)_2$, [**1**H]BAr$^F_4$, [**2**H]OMs, and [MoS(OTf)-(dmpe)$_2$]OTf. This material is available free of charge via the Internet at http//pubs.acs.org.

IC051443C